



Mud swimming: Locomotion through a viscoplastic fluid

Duncan Hewitt*

University College London, United Kingdom

ARTICLE INFO

Keywords:
Viscoplasticity
Locomotion
Swimming
Slender-body theory

ABSTRACT

Different classical models of small, slow (inertialess) swimming are considered when the ambient fluid has a yield stress. A variety of organisms inhabit and have to move through mud, mucus and other biological media, or more generally, soil and sand, all of which can exhibit viscoplastic behaviour. Basic mechanisms for inertialess swimming in 'simple' viscoplastic (Bingham) fluids are considered from a theoretical and numerical standpoint, with a particular focus on the role of the yield stress, the location of plugged-up regions around the swimmer's body, and the speed and efficiency of locomotion. Taylor's canonical 'swimming sheet', idealised versions of squirming organisms, and long, thin worm-like motions are all discussed, the latter of which involves a generalisation of classical slender-body theory for viscoplastic fluids.

Videos to this article can be found online at <https://doi.org/10.1016/j.sctalk.2022.100029>.

Figures and tables

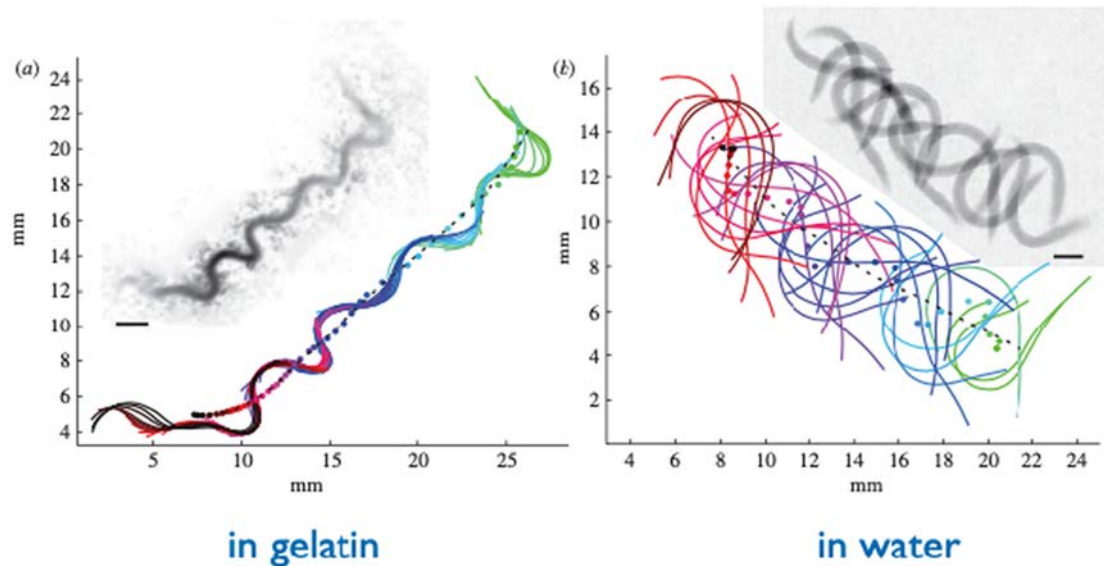


Fig. 1. Figure taken from [1]. Undulatory burrowing of the worm *Armandia brevis* in gelatin (left) and in water (right). The colors represent different snapshots in time, and the shadow-image is a series of overlaid snapshots. In gelatin, the worm 'burrows' along its own axis.

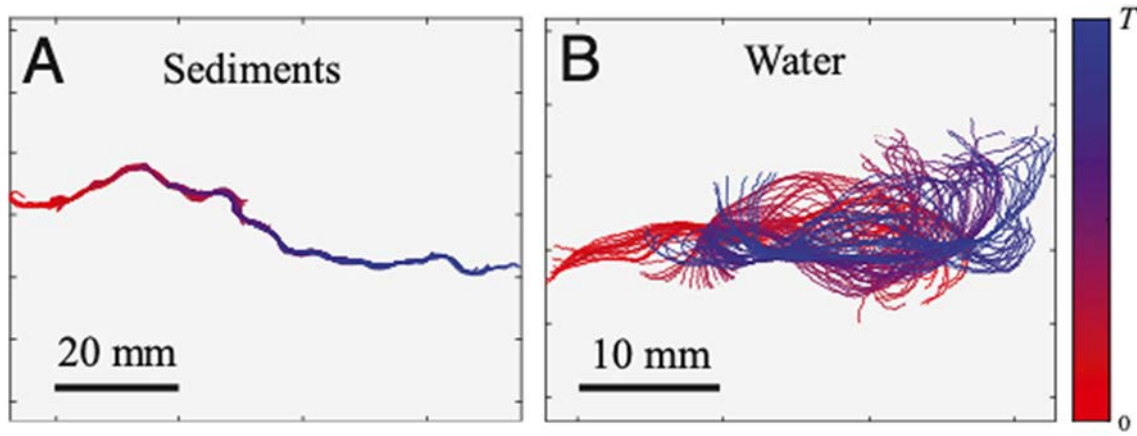


Fig. 2. Figure taken from [2]. Burrowing of earthworms by undulation and peristalsis, in sediment suspension (left) and water (right). Different colors again represent different snapshots in time.

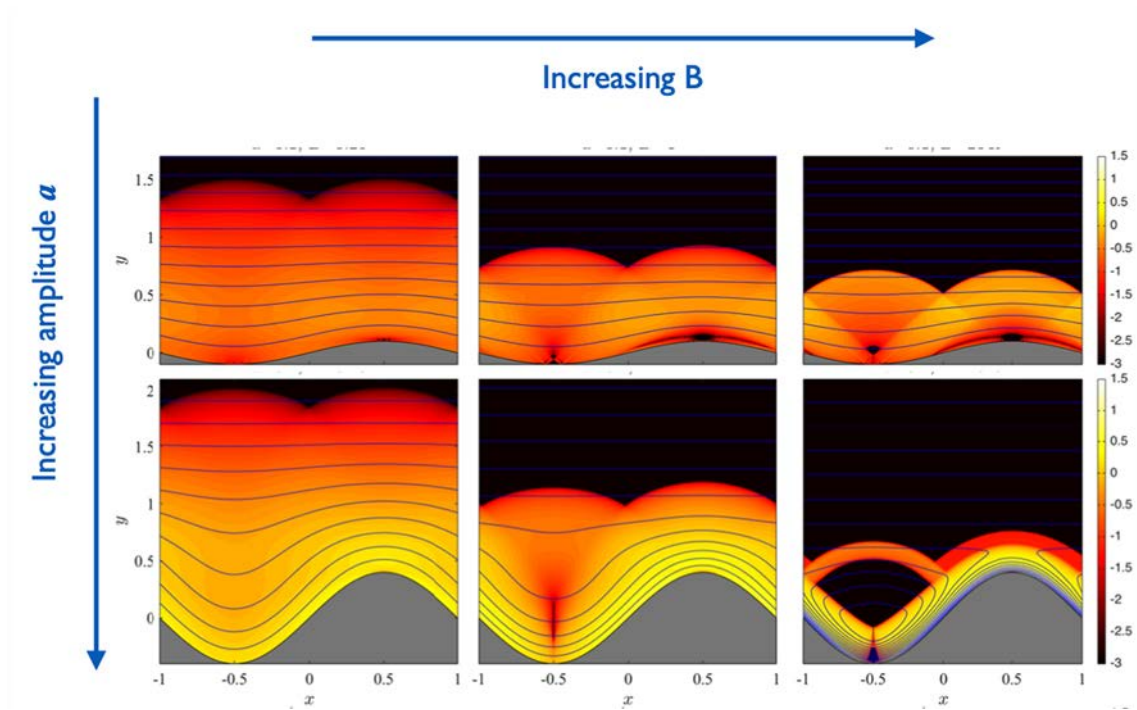


Fig. 3. Logarithm of the strain rate for Taylor's swimming sheet in a Bingham fluid, for varying amplitude a and Bingham number B . See [3] for further details.

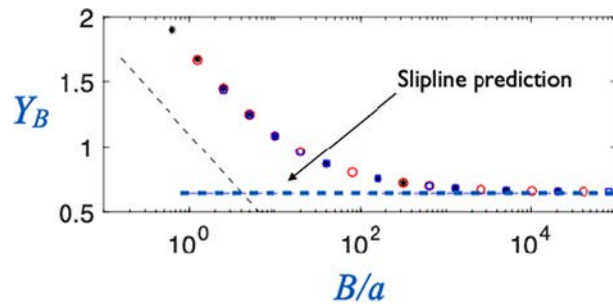


Fig. 4. The mean distance to the yield surface from the swimming sheet together with asymptotic predictions for large and small Bingham number; see [3] for further details.

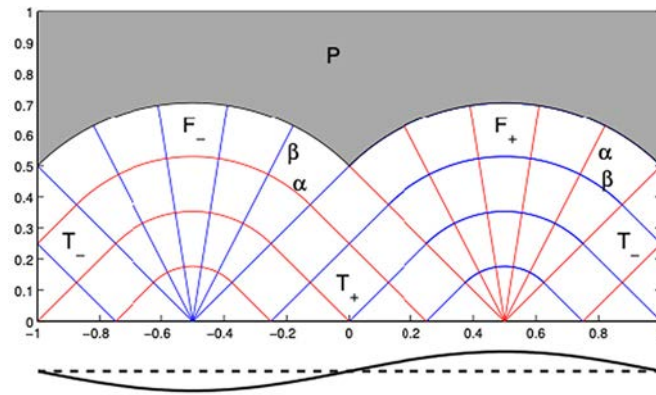


Fig. 5. Slipline solution for a perfectly plastic swimming sheet.

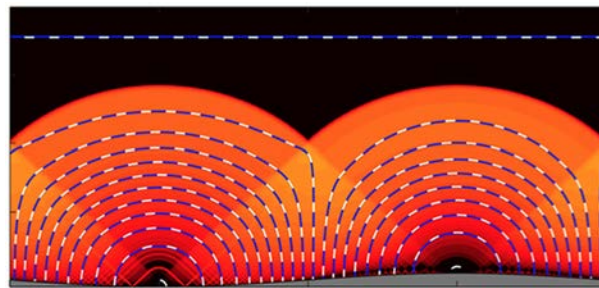


Fig. 6. Streamlines (blue) and strain rate for a low-amplitude, high Bingham number swimming sheet, together with predicted streamlines (dashed white) from slipline theory. (For interpretation of the references to colour in this figure legend, the reader is referred to the web version of this article.)

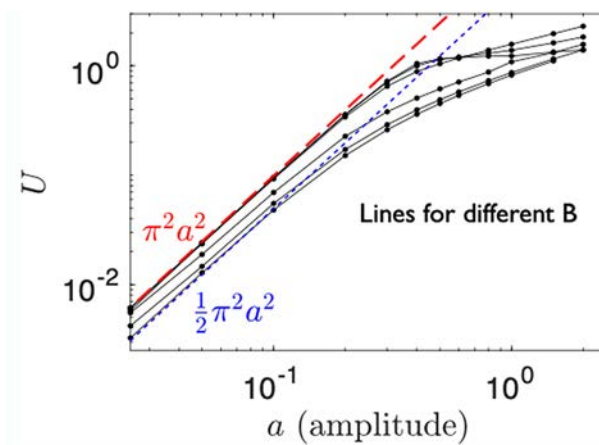


Fig. 7. Swimming speed against amplitude for the swimming sheet, for different Bingham numbers.

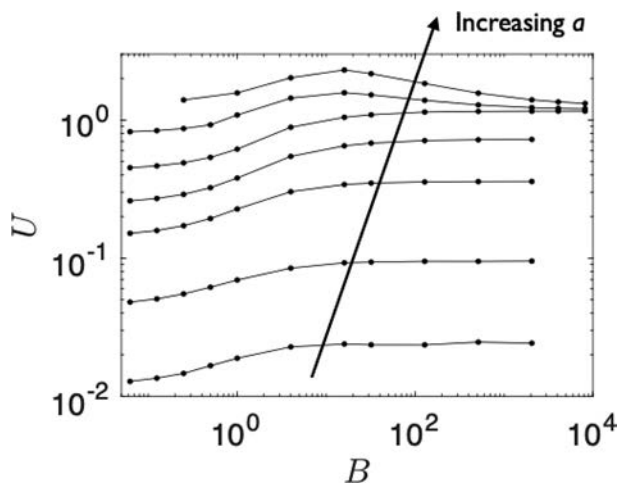


Fig. 8. Swimming speed against Bingham number for the swimming sheet, for different amplitudes.

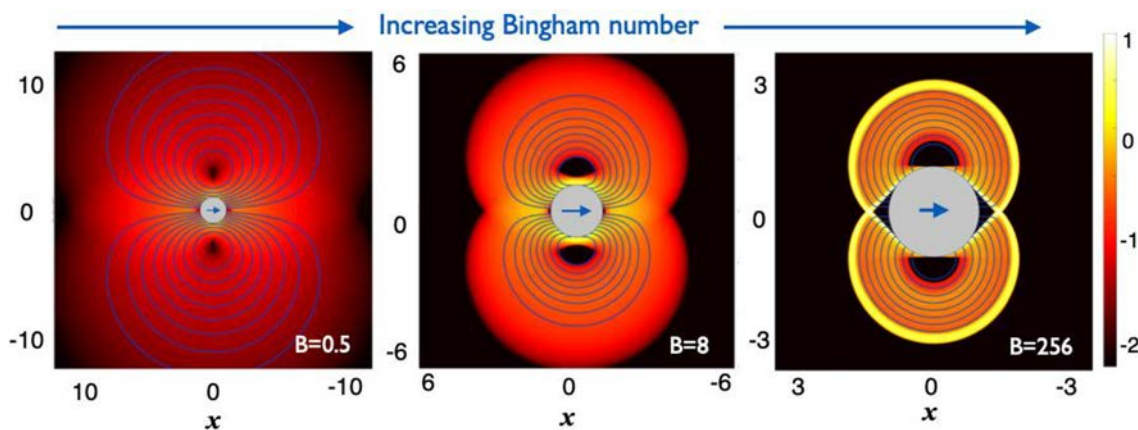


Fig. 9. Color plots of the logarithm of the strain rate, together with streamlines, around a translating cylinder for different Bingham numbers as marked. Black regions are undeformed plugs.

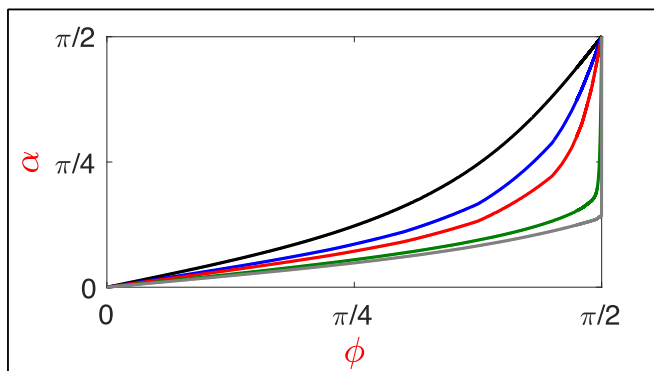


Fig. 10. The angle of the force against the angle of motion for increasing Bingham number from black through red to grey. For large Bingham number, there is a significant change in force angle over a very narrow range of motion angle near $\phi = \pi/2$. See [4] for further details. (For interpretation of the references to colour in this figure legend, the reader is referred to the web version of this article.)

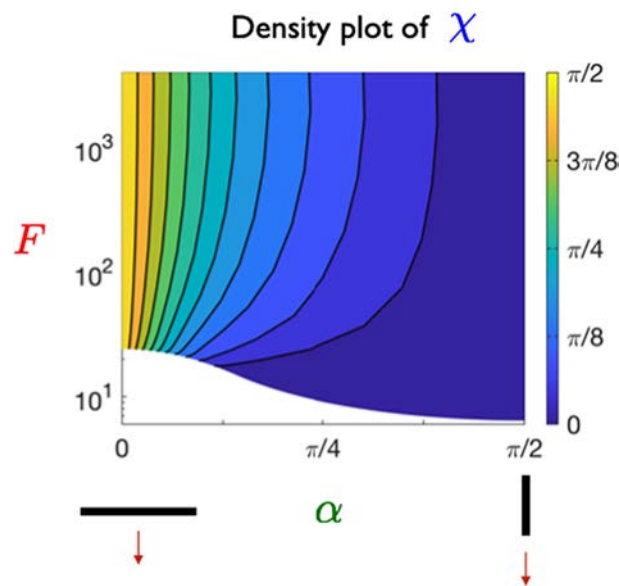


Fig. 11. Angle of motion for cylinders dropped at an angle α with a dimensionless weight F . The white region signifies no motion; see [4] for further details.

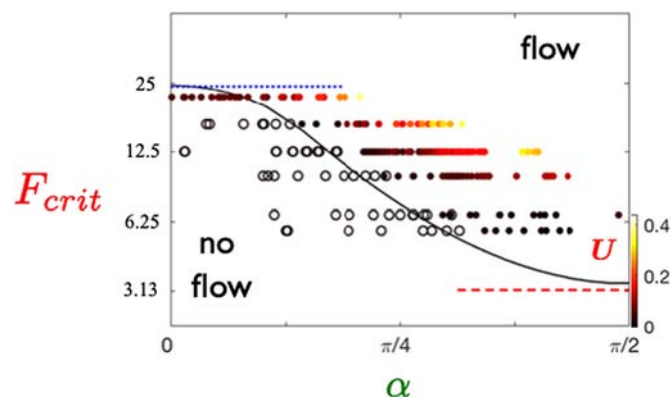


Fig. 12. Experiments with dropped cylinders in Carbopol gel, showing the speed of motion. Open symbols did not move. The line is the predicted boundary of motion (the edge of the white region in Fig. 11).

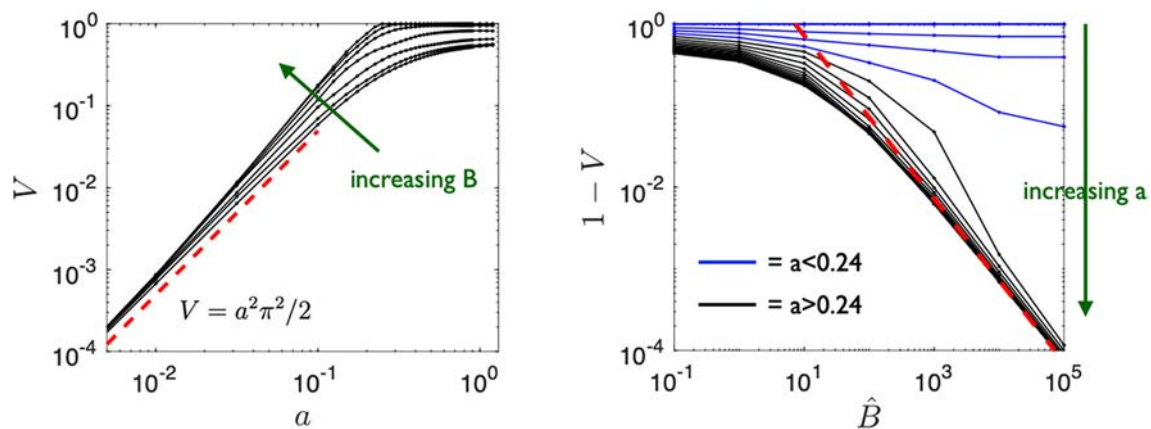


Fig. 13. Speed of undulating cylindrical filament moving in a Bingham fluid with Bingham number B and amplitude a , relative to the wave speed. When $a > 0.24$, the speed becomes very close to the wave speed ($V \approx 1$) for large enough Bingham number; see [5] for further details.

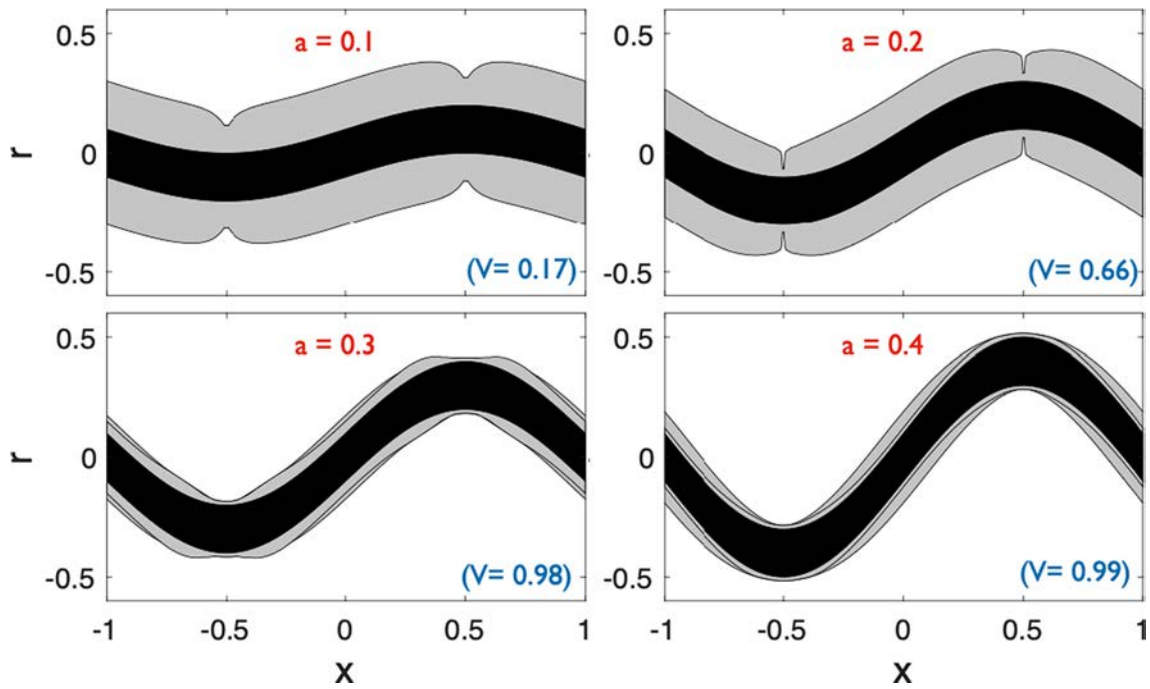


Fig. 14. Yield surfaces around cylindrical swimming filaments for different amplitude, at fixed Bingham number $B = 1000$. For large enough amplitude, the flow becomes very localized around the swimmer, which is able to ‘burrow’ almost along its axis at the wave speed; see [5] for further details.

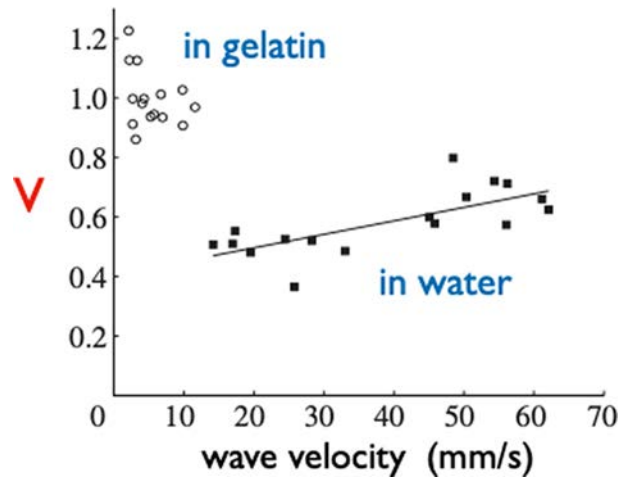


Fig. 15. Figure taken from [1]. The dimensionless swimming speed against the wave speed for the worm *armandia brevis*; in material with a yield stress, the worm burrows with $V \approx 1$, as in our theory.

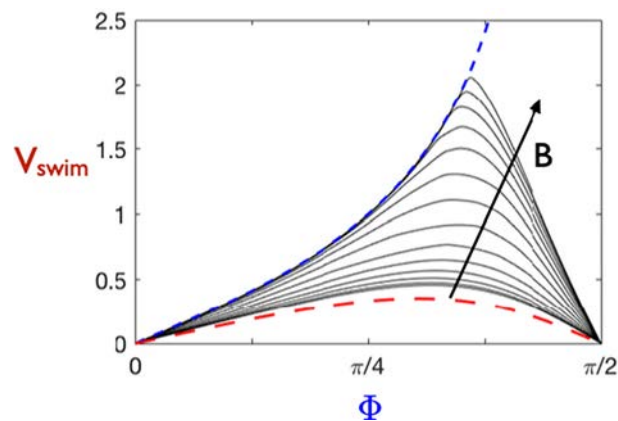


Fig. 16. Swimming speed (scaled by rotation speed) for a cylindrical helical swimmer, against the pitch angle of the helix. For large Bingham number, the filaments of the helix move almost along their axis (dashed blue line) for a wide range of pitch angle; see [4] for further details. (For interpretation of the references to colour in this figure legend, the reader is referred to the web version of this article.)

Acknowledgments

All of this work was carried out in collaboration with Neil Balmforth.

Funding

This research did not receive any specific grant from funding agencies in the public, commercial, or not-for-profit sectors.

Declaration of interests

The authors declare that they have no known competing financial interests or personal relationships that could have appeared to influence the work reported in this paper.

References

- [1] K.M. Dorgan, C.J. Law, G.W. Rouse, Meandering worms: mechanics of undulatory burrowing in muds, *Proc. R. Soc. B* 280 (20122948) (2013).
- [2] A. Kudrolli, B. Ramirez, Burrowing dynamics of aquatic worms in soft sediments, *PNAS* 116 (2019) 25569–25574.
- [3] D.R. Hewitt, N.J. Balmforth, Taylor's swimming sheet in a yield stress fluid, *J. Fluid Mech.* 828 (2017) 33–56.
- [4] D.R. Hewitt, N.J. Balmforth, Viscoplastic slender-body theory, *J. Fluid Mech.* 856 (2018) 870–897.
- [5] D.R. Hewitt, N.J. Balmforth, Locomotion with a wavy cylindrical filament in a yield-stress fluid, *J. Fluid Mech.* 936 (A17) (2022).